

## Effect of milling parameters on the phase transformations and morphology changes of B<sub>4</sub>C-SiC nanocomposite powder in situ synthesized by MAVCS method

Hamed Roghani<sup>a</sup>, Seyed Ali Tayebifard<sup>a,\*</sup>, Asghar Kazemzadeh<sup>a</sup> and Leila Nikzad<sup>b</sup>

<sup>a</sup>Semiconductor Department, Materials and Energy Research Center, Karaj, Iran

<sup>b</sup>Ceramic Department, Materials and Energy Research Center, Karaj, Iran

In this study, in situ synthesis of B<sub>4</sub>C-SiC nanocomposite powder (1 : 1 molar ratio) was performed by mechanically activated volume combustion synthesis (MAVCS) method. Raw materials were included Si, C, B<sub>2</sub>O<sub>3</sub> and Mg. Milling process was used to mechanically activate the raw materials. Synthesis of prepared samples was occurred in a tube furnace under argon atmosphere at 1000 °C. The milling parameters were examined to optimize the activating of the raw materials process. Synthesized samples after mechanical activation with milling parameters of 300 rpm rotation speed, 20 to 1 ball to powder ratio and milling time of 9 and 12 h had best phase and morphology conditions. Average crystallite size of B<sub>4</sub>C and SiC compounds were calculated less than 15 nm for these two samples. Transmission electron microscopy (TEM) analysis of these two samples approved their formation from the grains in nanometers scale. The TEM analysis showed the sample with 12 h of milling the raw materials has formed from more uniform grains than the sample with 9 h of milling the raw materials. Particle size analysis showed more than 99% of the particles from both samples have a size less than 1000 nm.

**Key words:** Volume combustion synthesis, Mechanical activation, B<sub>4</sub>C-SiC composite, nanocomposite powder, Phase evaluation, Morphology.

### Introduction

Boron carbide (B<sub>4</sub>C) due to the combination of its remarkable hardness, high melting temperature (~ 2743 K), low density (2.52 g.cm<sup>-3</sup>), wear resistance, chemical stability and neutron absorption capability is used in cutting tools, nuclear industry and thermodynamic applications [1-4]. Also, silicon carbide (SiC) due to properties such as high decomposition temperature (~ 3100 K), high hardness, chemical stability, high corrosion resistance and relatively low density (3.21 g.cm<sup>-3</sup>) is regarded in the industry and is used in many cases such as abrasives and cutting tools, electronic equipment and heating elements [4-7]. However, due to difficulty of sintering, SiC and B<sub>4</sub>C should be composed with other materials. B<sub>4</sub>C and SiC composites can improve the sinterability and the special properties of the two compounds [3, 8-10].

Combustion Synthesis (CS) is a highly exothermic reaction between components that self sustained through an entire sample. During this process, high speed heating and cooling of the sample causes various defects in the synthesized compound. Therefore, sintering temperature of the compounds produced by CS is less than the conventional methods. In some cases, entire sample is

heated uniformly until reaction occurs simultaneously throughout the sample volume. This mode of reaction entitled to volume combustion reaction (VCS) and is sometimes referred to as the thermal explosive mode. Some compounds need activation such as mechanical activation, chemical oven and preheat for spontaneous synthesis. Mechanical activation (MA) is a simple and appropriate method for activating the materials. Also the mechanical activation is required to achieve the nanocrystallites and nanocomposites. Due to the high reaction rate and the short time duration for increasing the sample temperature, the changes made by milling and deformation of the particles can have its effect even after synthesis on the microstructure [5, 11-15].

Reduction of boron oxide (B<sub>2</sub>O<sub>3</sub>) by magnesium (Mg) will cause the production of magnesium oxide (MgO) in products. In various studies leaching with hydrochloric acid (HCl) in different concentrations and times has been used to remove MgO [1, 15-17].

In this study, in situ synthesis of B<sub>4</sub>C-SiC nanocomposite by mechanically activated volume combustion synthesis (MAVCS) method has been investigated. Mechanical activation by milling has been used to activate the mixture of raw materials and improve synthesis conditions. The effect of milling variables such as ball to powder ratio and milling time on the synthesis methods, phase transformations and morphology changes have been investigated and optimum condition for milling has been obtained.

\*Corresponding author:  
Tel : +98-26-36280042  
Fax: +98-26-36280030  
E-mail: a\_tayebifard@yahoo.com

## Experimental

### Preparation

Raw materials including Si (>99% purity and particle size  $\approx 150 \mu\text{m}$ ), graphite (99.5% purity and particle size  $\approx 50 \mu\text{m}$ ) and Mg powders (>99% purity and particle size  $< 100 \mu\text{m}$ ) and 37% HCl ( $\approx 99\%$  purity) manufactured by Merck and B<sub>2</sub>O<sub>3</sub> powder (>99% purity and particle size  $< 50 \mu\text{m}$ ) manufactured by SDFCL Co. One mol excess Mg from the stoichiometric quantity (Eq. (1)) was used as a result of evaporation of Mg during combustion [15]. Weighed materials were milled by Retsch PM100 planetary mill with 250 ml steel cup under argon atmosphere, according to milling parameter of Table 1. Tablet shape samples with 10 mm diameter and 5 mm height were prepared from the milled powders by uniaxial cold press. The combustion reactions were carried out in tubular furnace under a continuous argon gas flow at 1000 °C. Combustion temperature at some of samples reaction was measured by optical pyrometer, which was focused on the sample.



$$\Delta H_r^\circ = -1232 \text{ kJ}\cdot\text{mol}^{-1}, H_r^\circ = -1207.922 \text{ kJ}\cdot\text{mol}^{-1}$$

After synthesis, leaching by HCl used to removing MgO and the other unwanted products according Eq. (2) [17]. 0.3 g of combustion product of each sample was leached by 30 ml of 1 molar hydrochloric acid for 1 h at 80 °C.



### characterization

The phase compositions of samples were determined by X-ray diffraction (XRD) (Philips PW 3710, Cu K $\alpha$  and radiation at 0.8 °/min scanning rate) and the average crystallite size and microstrain determined by Rietveld analysis [18]. The morphology of samples was characterized by scanning electron microscopy (SEM,

Cambridge S360) and the transmission electron microscope (TEM, Philips CM30). The particle size of leached sample with appropriate phase and morphology was determined by Zetasizer instrument (Malvern 3000HSA).

## Results and Discussion

The reaction of B<sub>2</sub>O<sub>3</sub> reduction by Mg and the formation of B<sub>4</sub>C-SiC composites (Eq. (1)) have an appropriate adiabatic temperature (2750 K, calculated by Eq. (3)) according to the executable criteria of combustion reaction [11, 19]. Nevertheless, standard formation enthalpy of B<sub>4</sub>C and SiC are low. Therefore, activation process such as mechanical activation is required to the synthesis of B<sub>4</sub>C-SiC composite by VCS method [5, 15, 20]. Milling for mechanical activation is valid until a new phase during milling is not synthesized in appreciable amounts [21]. Researches confirm the milling process by parameter of Table 1 is appropriate and no phase synthesis during mechanical activation [22].

$$\Delta H_r^\circ = \int_{298K}^{T_{rd}} \sum n C_p(\text{products}) dT \quad (3)$$

### Investigating of ball to powder ratio effect

Fig. 1 shows the XRD patterns of milled samples after synthesis and leaching with a different ball to powder ratio. These XRD patterns prove that the leaching process has successfully eliminated MgO (byproduct of reduction of B<sub>2</sub>O<sub>3</sub> according to Eq. (1)). The leaching process can be represented by reaction Eq. (2) [15, 17].

Some unreacted C and Si can be seen in the XRD pattern of the sample with a ball to powder ratio of 10 to 1 (M324). Silicon phase is not observed and the carbon peak is considerably decreased and also a greater number of B<sub>4</sub>C peaks are visible by increase of ball to powder ratio to 15 to 1 (M334). As the ball to

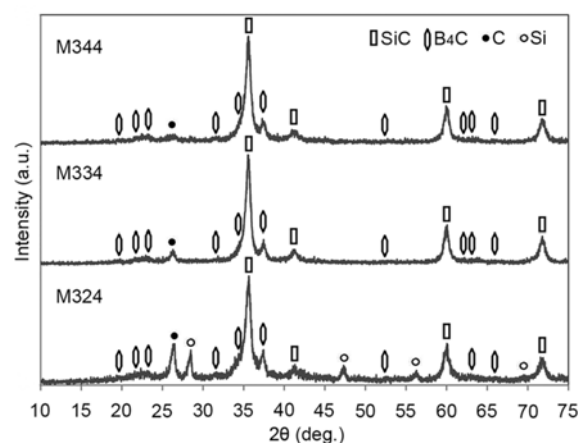


**Fig. 1.** XRD patterns of synthesized and leached unmilled sample (M0) and samples that milled their reactant by 10 (M324), 15 (M334) and 20 (M344) to 1 ball to powder ratio.

**Table 1.** Milling parameters of samples\*

Sample code	Rotation speed (rpm)	Ball to powder ratio	Milling time (h)
M0	–	–	0
M324	300	10	12
M334	300	15	12
M344	300	20	12
M341	300	20	3
M342	300	20	6
M343	300	20	9

\*At the samples code number one, two and three are 1/100 rotation speed, 1/5 ball to powder ratio and 1/3 milling time respectively

powder ratio increase in the M344 sample (ball to powder ratio of 20 to 1), C peak shows a more decrease, but there is no other difference between the diffraction pattern of this sample and the M334 sample. It can be claimed that the condition of the leached product has been closed to the steady state. Decreasing in the intensity of C peak in M344 compared to M334 could be due to the increasing of ball to powder ratio and as a result increasing in milling energy and microstrain and decreasing of crystallites size.

The average of the microstrain and crystallite size of the M324, M334 and M344 samples has calculated by Rietveld analysis and the results have listed in Table 2. The microstrain has been increased and the average of crystallite size has been decreased by increasing of the

**Table 2.** Average microstrain and crystallite size of the samples.

Sample code	Microstrain (%)		Crystallite size (nm)	
	B <sub>4</sub> C	SiC	B <sub>4</sub> C	SiC
M324	0.220	0.143	12.3	14.5
M334	0.480	0.170	10.8	13.3
M344	0.849	0.254	10.0	11.0
M341	0.321	0.114	12.2	14.0
M342	0.687	0.120	11.7	13.6
M343	0.733	0.174	9.0	11.0

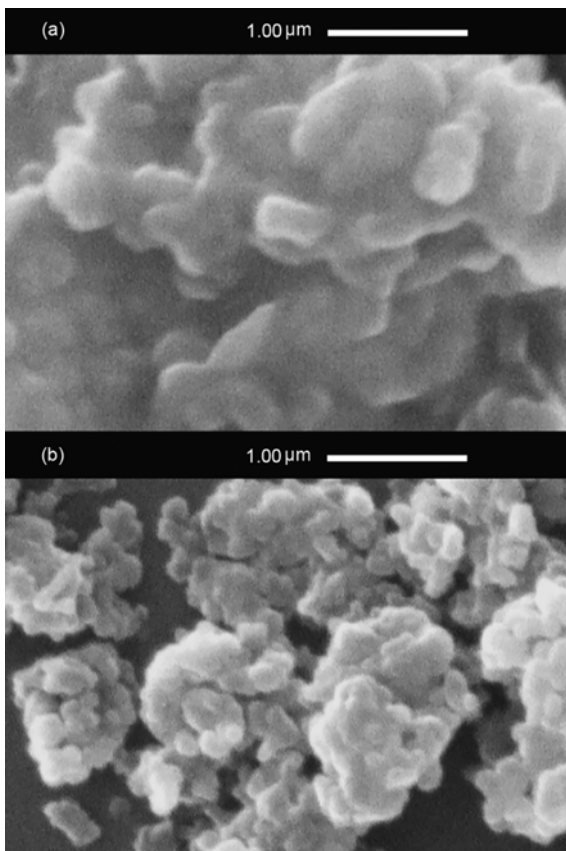


**Fig. 2.** SEM micrograph of synthesized and leached sample: (a) milled with ball to powder ratio 15 to 1 (M334); and (b) milled with ball to powder ratio 20 to 1 (M344).

ball to powder ratio and thus increasing of the milling energy. Also the crystallite size of the synthesized B<sub>4</sub>C-SiC composite of the all samples of this part has been calculated less than 15 nm.

SEM micrographs of the M334 and M344 samples is shown in Fig. 2. In Fig. 2(a) can be seen that M334 is formed from large particles by agglomeration of smaller particles. Also it is visible that a liquid phase surrounding the particles and their constituent grains and has caused them to be more adhesive. Only three phases of B<sub>4</sub>C, SiC and C are recognizable in the XRD analysis of M334. The adiabatic temperature of B<sub>4</sub>C-SiC composite formation reaction is 2750 K (calculated by Eq. (3) [19]) and the melting temperature of SiC, B<sub>4</sub>C, Si and B<sub>2</sub>O<sub>3</sub>, respectively, are ~ 3100 K, 2743 K, 1685 K and 723 K [4]. It can be understood that the sighted liquid phase is the unreacted raw materials according to the lower combustion temperature than the adiabatic temperature (due to the energy loss), visibility of residual carbon and lack of existence of transition phase in the product.

SEM micrograph of M344 (Fig. 2 (b)) indicates that this sample is consist of agglomerated particles with a size of submicron. Comparing the SEM micrographs of M334 with M344 shows the constituent particles of the M344 sample are smaller. Also there is no liquid phase in the grains and particles of this sample and agglomeration and adhesion are less. More ball to powder ratio and more energy of milling caused to more complete synthesis and eliminate of liquid phase.

The Mechanical activation by milling cause to intermix and homogeneity of weighed materials and decrease size of particles, grains and crystallites [13, 23]. According Eq. (1), at first, Mg reduce B<sub>2</sub>O<sub>3</sub> and then B<sub>4</sub>C-SiC composite form due to heat of reduction reaction. Also, MgO is about 72 wt% of the reaction product of Eq. (1). Appears to reduce the grain size and high homogeneity caused by milling, high rate combustion reaction and the formation of B<sub>4</sub>C and SiC in a network of the MgO, cause to increase nucleation and prevent grain growth. Therefore, composite formed from particles, grains and crystallites with nanometric size.

### Investigating of milling time effect

The ignition time diagram of samples with different milling time has been shown in Fig. 3. It is seen that the starting time of the ignition has been decreased significantly by increasing of milling time, so that this time has been reduced to about 1/3 from the sample without milling to the sample with 9 h milling. Decreasing in the starting time of ignition is due to finer grains and more energy of milled raw materials [13-15].

Fig. 3 shows by increasing the milling time from 9 to 12 h, the starting time of ignition has been increased slightly. This small amount of difference could be due

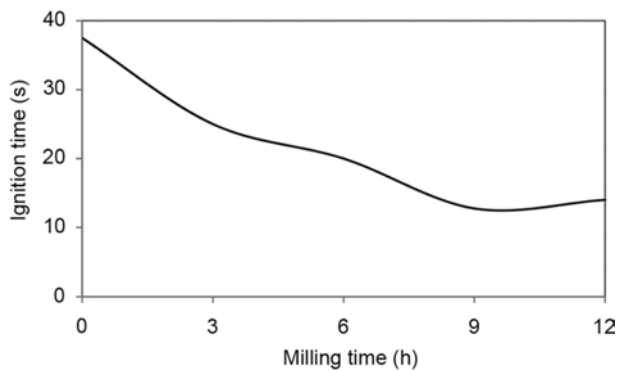


**Fig. 3.** The ignition time diagram of samples with different milling time.

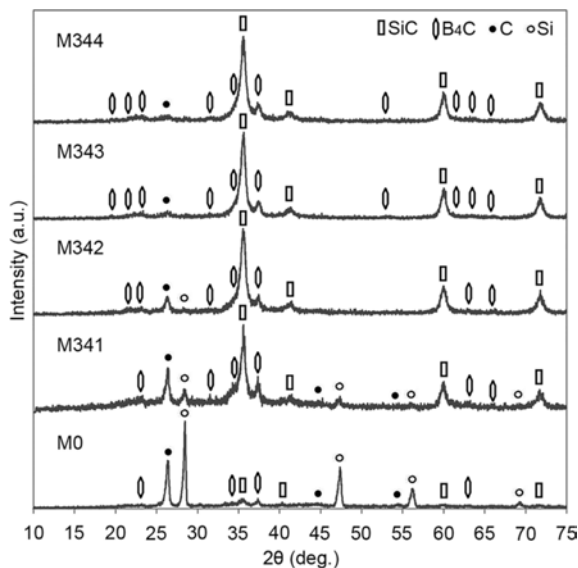


**Fig. 4.** XRD pattern after synthesis and leaching of the milled samples at: 0 h (M0); 3 h (M341); 6 h (M342); 9 h (M343); and 12 h (M344).

to the experimental error or the synthesis of a small amount of raw materials during the milling and its decelerative effect during the combustion synthesis [11, 24]. It can be concluded that the ignition time has reached to a relative equilibrium by the 9 h milling.

Fig. 4 shows the XRD patterns after synthesis and leaching of the milled samples with different milling times (from 0 to 12 h). Synthesized phases of B<sub>4</sub>C and SiC peaks are observed in the diffraction pattern of the sample without milling. Yet the intensity of these peaks are low and the peaks of unreacted raw materials are visible with a much more intensity. The synthesis of B<sub>4</sub>C-SiC composite has considerably intensified by milling. The peaks intensities of unreacted materials have been decreased considerably in the M341 sample.

The peaks intensity of synthesized B<sub>4</sub>C-SiC composite and residual materials of M341 are comparable with M324. This means that can achieve similar results by doubling the ball to powder ratio and decreasing of the milling time to a quarter. Therefore, increasing of the ball to powder ratio is more effective than increasing of

the milling time.

More B<sub>4</sub>C peaks are seen and the residual materials have decreased by further milling in M342. The Si phase peak is not seen by 9 h of milling in the XRD pattern of M343 and only the first peak of C is visible with low intensity. There is no difference in appearance between the diffraction patterns of the M343 and M344 samples.

The combustion temperature increases with milling according to the diagram of combustion temperature of the milled samples at different times (Fig. 5). More synthesis of desired compounds and decreasing in residual materials (according to the diffraction patterns in Fig. 4) that act as a consumer of energy, cause to the combustion temperature increases [15]. The samples reach the maximum combustion temperature by 6 to 9 h of raw materials milling and the combustion temperature decrease with a low gradient after 9 h. Synthesizing of a small amount of raw materials within the milling container can cause to decrease the combustion temperature after 9 h milling. According to thermodynamic data, the reduction of B<sub>2</sub>O<sub>3</sub> and forming of MgO during the milling is more probable [4].

It is seen in Table 2 that increasing the milling time has increased the average microstrain and decreased the average crystallite size. It can be mentioned that increasing in the microstrain in comparison of decreasing in the crystallites size of B<sub>4</sub>C-SiC composite compounds is more considerable. Increasing in milling has increased the microstrain more than 2 times, while the crystallite size has decreased about 0.2 times. It can be seen an increase and a meaningful difference between the average of calculated microstrain for M343 and M344 but calculations of the average crystallite size doesn't show significant difference. It can be understood that these two samples were in an appropriate condition of synthesis and average crystallite size.

Fig. 6 shows a SEM micrograph of the M343 and

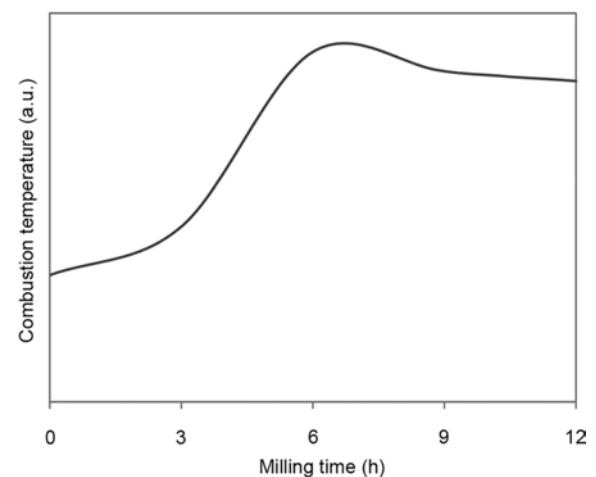


**Fig. 5.** Diagram of combustion temperature of milled samples in different reactant milling times.

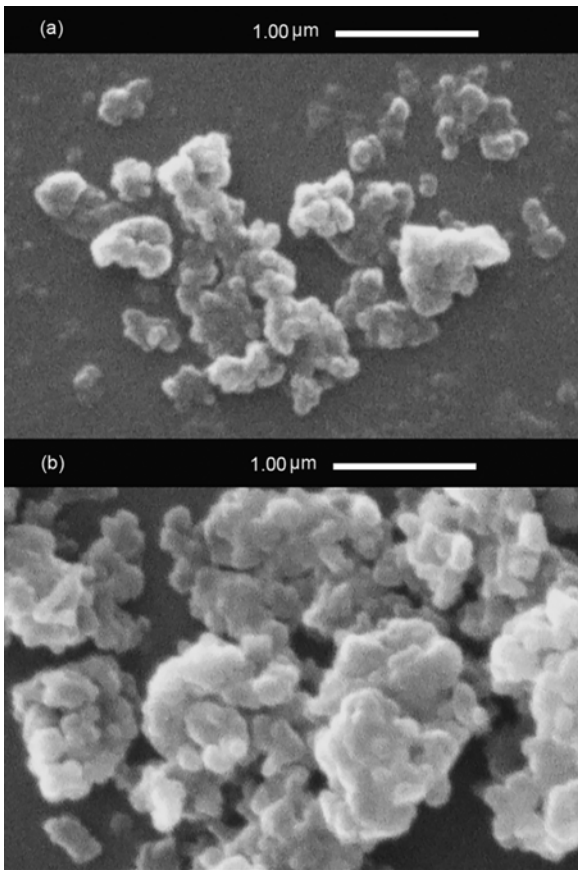


**Fig. 6.** SEM micrograph after synthesis and leaching of the reactant milled samples at: (a) 9 h (M343); (b) 12 h (M344).

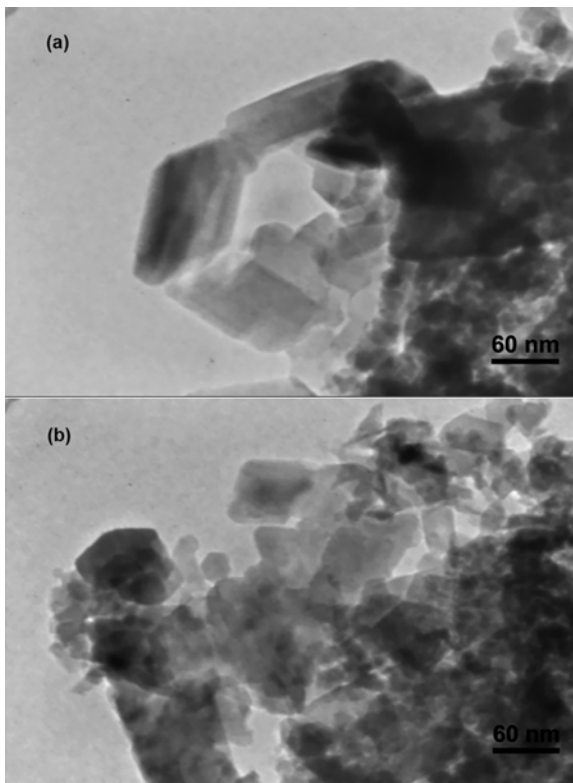


**Fig. 7.** TEM image after synthesis and leaching of reactant milled samples at: (a) 9 h (M343); (b) 12 h (M344).

M344 samples after leaching. Both samples have formed of polyhedral agglomerated particles with submicron dimensions (often less than 200 nm). Also size and shape of the grains are fairly homogeneous.

Fig. 7 shows the TEM image of the M343 and M344 samples after leaching. M343 has larger grains in its structure compared to M344 and M344 is more homogeneous in grain size rather than M343. This could be due to the higher milling time of M344. Nevertheless, both samples consist of nanometric grains so that the grain size seen in the TEM analysis were often less than 30 nm for M344 and the maximum grain size in M343 had 70 nm width and about 100 nm length. Also the nanometric grain size of the two mentioned samples confirms the average crystallite size calculated by Rietveld analysis.

Fig. 8 shows the particle size diagram based on the number of particles for M343 and M344 after the synthesis process and leaching. The information on this diagram are listed in Table 3. As it is seen in Fig. 8 and Table 3, the most particles of the synthesized  $B_4C$ -SiC nanocomposite (more than 99%) have a size less than 1000 nm. This approves the synthesizing of ultrafine nanocomposite powder of  $B_4C$ -SiC. The both samples have a means size of about 100 nm and 400 nm. Yet the percentage of particles with a size of 100 nm and less are significantly higher in M344 (12 h of milling) compared to M343 (9 h of milling). This is consistent with the results of TEM analysis which can be due to the further milling of M344 before synthesis process. M343 shows a greater percentage of particles between 100 to 500 nm and the particles percentage under 500 and 1000 nm are slightly more in this sample. The existence of particles with different submicron size is caused the improvement of sinterability in the both samples. Hence, the synthesized  $B_4C$ -SiC nanocomposite is an appropriate choice using to sintering a sample [25].

In spite of a more homogeneous microstructure of

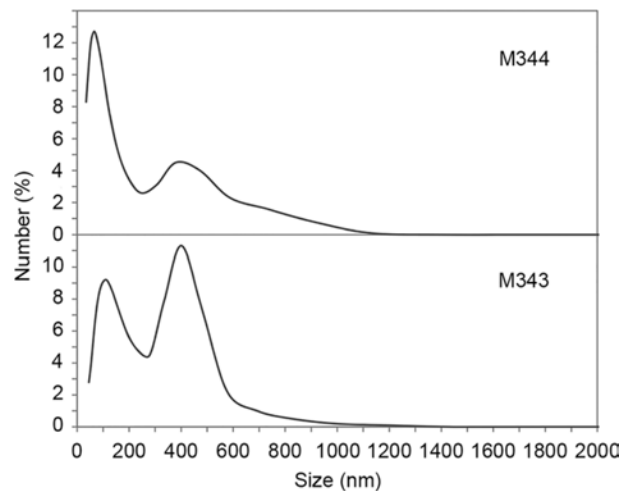


**Fig. 8.** Particle size diagram based on the number of particles for synthesized and leached samples after reactant milling at: 9 h (M343); 12 h (M344).

**Table 3.** Data of the particle size diagram based on the number of particles of the M343 and M344 samples after synthesis and leaching (Fig. 9).

Means (nm)		Sample code	Number of particles (%)		
			≤ 1000 nm	< 500 nm	< 100 nm
418.1	130.0	M343	99.9	96.5	38.8
452.1	87.3	M344	99.7	95.0	64.9

M344, components of M343 are in the nanometric range too. According to this reason and the similar synthesis results of these two samples, milling terms for the M343 sample can be considered as the optimal conditions due to 3 h of less milling.

### Conclusions

B<sub>4</sub>C-SiC nanocomposite powder (1 : 1 molar ratio) was successfully synthesized by mechanically activated volume combustion synthesis (MAVCS) method. The M343 and M344 samples with 300 rpm rotation speed, ball to powder ratio of 20 to 1 and milling time of 9 and 12 h had a good condition of synthesis and microstructure. The average crystalline size of B<sub>4</sub>C and SiC compounds was calculated less than 15 nm for these two samples. TEM analysis was approved the formation of grains in nanometric scale for these two samples. TEM analysis revealed that M344 with 12 h of milling compared to M343 with 9 h of milling has formed of the grains with more uniform size. More than 99% of particles in the both samples had the size less than 1000 nm in the grain size analysis. Also 38.8% of M343 particles and 64.9% of M344 particles have a dimension about 100 nm and less. The calculated average crystallite size, TEM images and the results of the particles size analysis approve the synthesizing of B<sub>4</sub>C-SiC nanocomposite and producing of nanocomposite powder in nanometer scale.

### References

1. F. Deng, H.Y. Xie and L. Wang, *Mater. Lett.* 60[13-14] (2006) 1771-1773.
2. E. Mohammad Sharifi, F. Karimzadeh and M.H. Enayati,

3. L. Nikzad, T. Ebadzadeh, M.R. Vaezi and A. Tayebifard, *J. Ceram. Process. Res.* 13[5] (2012) 590-594.
4. I. Barin, "Thermochemical Data of Pure Substances" (VCH, 1995).
5. H.-B. Jin, J.-T. Li, M.-S. Cao and S. Agathopoulos, *Powder Technol.* 196[2] (2009) 229-232.
6. A. Morançais, F. Louvet, D.S. Smith and J.-P. Bonnet, *J. Eur. Ceram. Soc.* 23[11] (2003) 1949-1956.
7. P. Rai, J.-S. Park, G.-G. Park, W.-M. Lee, Y.-T. Yu, S.-K. Kang, S.-Y. Moon and B.-G. Hong, *Adv. Powder. Technol.* 25[2] (2014) 640-646.
8. G. Liu, J. Li, Y. Shan and J. Xu, *Scripta Mater.* 67[4] (2012) 416-419.
9. F.C. Sahin, B. Apak, I. Akin, H.E. Kanbur, D.H. Genckan, A. Turan, G. Goller and O. Yucel, *Solid State Sci.* 14[11-12] (2012) 1660-1663.
10. Z. Zhang, X. Du, J. Wang, W. Wang, Y. Wang and Z. Fu, *Powder Technol.* 254[0] (2014) 131-136.
11. J.J. Moore and H.J. Feng, *Prog. Mater. Sci.* 39[4-5] (1995) 243-273.
12. S.T. Aruna and A.S. Mukasyan, *Curr. Opin. Solid. St. M.* 12[3-4] (2008) 44-50.
13. L. Takacs, *Prog. Mater. Sci.* 47[4] (2002) 355-414.
14. P. Mossino, *Ceram. Int.* 30[3] (2004) 311-332.
15. L. Nikzad, T. Ebadzadeh, M.R. Vaezi and A. Tayebifard, *Micro Nano Lett. IET* 7[4] (2012) 366-369.
16. Z. Zhang, X. Du, W. Wang, Z. Fu and H. Wang, *Int. J. Refract. Met. H.* 41[0] (2013) 270-275.
17. U. Demircan, B. Derin and O. Yücel, *Mater. Res. Bull.* 42[2] (2007) 312-318.
18. X'Pert HighScore Plus (PANalytical B.V, 2006) 2.2b edn.
19. Z.A. Munir and U. Anselmi-Tamburini, *Materials Science Reports*, 3[7-8] (1989) 277-365.
20. K. Yang, Y. Yang, Z.-M. Lin, J.-T. Li and J.-S. Du, *Mater. Res. Bull.* 42[9](2007) 1625-1632.
21. L. Nikzad, R. Licheri, M.R. Vaezi, R. Orrù and G. Cao, *Int. J. Refract. Met. H.* 35[0] (2012) 41-48.
22. H. Roghani-Mamaghani, A. Tayebifard, A. Kazemzadeh and L. Nikzad, in "Preparation of SiC-B<sub>4</sub>C Nanocomposite by SHS Method by Combining Mechanical Activation and Magnesium-Thermite Processes" M.Sc. Thesis (Materials and Energy Research Center, 2014).
23. C. Suryanarayana, *Prog. Mater. Sci.* 46(2001) 184.
24. Y. Yang, K. Yang, Z.-M. Lin and J.-T. Li, *Mater. Lett.* 61[3] (2007) 671-676.
25. L.L. Hench and G.Y. Onoda, "Ceramic Processing before Firing" (Wiley-Interscience, 1978).